

# Extreme mid-winter drought weakens tree hydraulic–carbohydrate systems and slows growth

J. Mason Earles<sup>1</sup> , Jens T. Stevens<sup>2</sup> , Or Sperling<sup>3</sup>, Jessica Orozco<sup>4</sup>, Malcolm P. North<sup>4,5</sup> and Maciej A. Zwieniecki<sup>4</sup>

<sup>1</sup>School of Forestry & Environmental Studies, Yale University, New Haven, CT 06511, USA; <sup>2</sup>Department of Environmental Science, Policy and Management, University of California Berkeley, 145 Mulford Hall, Berkeley, CA 94720, USA; <sup>3</sup>Volcani Center, Agricultural Research Organization, M.P. Negev 85280, Israel; <sup>4</sup>Department of Plant Sciences, University of California Davis, One Shields Ave, Davis, CA 95616, USA; <sup>5</sup>USDA Forest Service, PSW Research Station, 1731 Research Park Dr., Davis, CA 95618, USA

## Summary

Author for correspondence:

J. Mason Earles

Tel: +1 415 870 0204

Email: j.earles@yale.edu

Received: 27 October 2017

Accepted: 28 February 2018

*New Phytologist* (2018) **219**: 89–97

doi: 10.1111/nph.15136

**Key words:** climate change, drought, forest, hydraulics, stress, water, winter.

- Rising temperatures and extended periods of drought compromise tree hydraulic and carbohydrate systems, threatening forest health globally. Despite winter's biological significance to many forests, the effects of warmer and dryer winters on tree hydraulic and carbohydrate status have largely been overlooked.
- Here we report a sharp and previously unknown decline in stem water content of three conifer species during California's anomalous 2015 mid-winter drought that was followed by dampened spring starch accumulation. Recent precipitation and seasonal vapor pressure deficit (VPD) anomaly, not absolute VPD, best predicted the hydraulic patterns observed.
- By linking relative water content and hydraulic conductivity ( $K_h$ ), we estimated that stand-level  $K_h$  declined by 52% during California's 2015 mid-winter drought, followed by a 50% reduction in spring starch accumulation. Further examination of tree increment records indicated a concurrent decline of growth with rising mid-winter, but not summer, VPD anomaly.
- Thus, our findings suggest a seasonality to tree hydraulic and carbohydrate declines, with consequences for annual growth rates, raising novel physiological and ecological questions about how rising winter temperatures will affect forest vitality as climate changes.

## Introduction

### Drought seasonality and its impact on forest health

Drought has a major influence on global forest distribution and community composition. Moreover, drought can substantially lower net primary productivity (Zhao & Running, 2010), intimately linking it to the global carbon cycle. Forest die-off events are increasing due to synergistic effects of drought, climate change, and land management practices (Allen *et al.*, 2015; Young *et al.*, 2017), leading to vegetation conversion (Allen & Breshears, 1998; Fellows & Goulden, 2012) and cascading effects at the ecosystem level (van der Molen *et al.*, 2011; Millar & Stephenson, 2015). In particular, droughts are projected to increasingly coincide with rising temperatures that can exacerbate the physiological stress experienced by trees during drought due to increasing potential evapotranspiration with limited water availability (Allen *et al.*, 2010; Adams *et al.*, 2017). However, despite the importance of temperature to drought physiology in plants, ecological models of vegetation change rarely incorporate seasonal variation in climate (Keeley & Syphard, 2016), typically focusing on the vegetative part of the season.

A primary cause of tree mortality during drought is hydraulic failure (Breshears *et al.*, 2009; Anderegg *et al.*, 2012), which occurs as embolism forms within plant vascular conduits in response to water stress. Embolism reduces a plant's capacity to transport water from soil to leaves, limiting photosynthetic activity, affecting its carbohydrate reserves, and increasing the likelihood of mortality. The risk of hydraulic failure in plant vascular tissue is in part determined by soil water availability and atmospheric water demand, which together create the water potential gradient between soil and atmosphere. Atmospheric water demand is measured by vapor pressure deficit (VPD), a function of concurrent temperature and relative humidity, which dictates the evaporative demand imposed on plant leaves (Park Williams *et al.*, 2012; Jensen *et al.*, 2016). High VPD, combined with low precipitation, results in low water availability and increases the risk of hydraulic failure in plants.

Nonstructural carbohydrate (NSC) depletion is another primary mechanism thought to underlie tree mortality during drought (McDowell *et al.*, 2008; Sevanto *et al.*, 2014; Adams *et al.*, 2017). Specifically, drought is thought to induce extended periods of stomatal closure that eventually shift a plant from excess carbohydrate production to excess demand, which draws upon insoluble NSC reserves (i.e. starch) (McDowell *et al.*,

2008). Starch reserves are consequently expected to increase during periods of high transpiration/photosynthesis and decrease in response to limited photosynthetic activity (McDowell *et al.*, 2008). Thus, high VPD, combined with low precipitation, not only increases the risk of hydraulic failure, but also carbohydrate depletion and potential starvation.

In temperate climates, absolute VPD is highest in the summer because it is strongly dependent on temperature, and therefore the risk of hydraulic failure is generally presumed highest during the summer as well (Nardini *et al.*, 2013). Indeed, high summer VPD (i.e. high temperature and low relative humidity) and water scarcity correspond well with decreased productivity and elevated mortality in southwestern US forests (Park Williams *et al.*, 2012). However, in Mediterranean-climate forests, which are defined by mild-wet winters and warm-dry summers, the period of highest VPD (summer) is consistently decoupled from the period of highest water availability (winter), and many evergreen trees in these climates can photosynthesize and grow year-round (Kelly & Goulden, 2016). This decoupling raises the possibility that many trees may be more sensitive to increased winter temperatures than summer temperatures under drought conditions, despite lower absolute winter VPD, a hypothesis that has not been explicitly tested before.

Recent winter drought in California and other Mediterranean-climate regions have been characterized not only by very low precipitation, but also by record-setting warm winter temperatures (Robeson, 2015; Williams *et al.*, 2015; Young *et al.*, 2017). In 2015, California experienced an anomalously warm mid-winter drought, where precipitation in our study area from January through March – historically the three wettest months in the region – was 75% below the prior 110-yr mean, and temperatures were 45% above the prior 110-yr mean (Menne *et al.*, 2015). These conditions provided a valuable opportunity to examine the effects of warming winter temperatures under drought conditions on tree hydraulics and carbohydrate status. Despite its potential ecological significance, the effect of high winter VPD coincident with reduced winter precipitation on plant hydraulic and carbohydrate status is not well understood.

In this study we examined how California's extreme 2015 mid-winter drought affected the hydraulic and carbohydrate status of three species of evergreen conifer trees by periodically monitoring relative water content (RWC) and soluble/insoluble NSCs over eighteen months. To determine how climatic conditions affected tree hydraulic status, we modeled RWC as a function of recent precipitation and VPD anomaly. We then used the strong relationship between branch-level RWC and hydraulic conductivity to infer historic changes in hydraulic conductivity at our site for both winter and summer months from 1992 into 2015. We also compared the degree of spring NSC accumulation following the anomalous 2015 mid-winter drought to the prior year's accumulation. Finally, we investigated how the physiological changes above might affect tree growth by measuring the relative growth rate (ring-width index) of our study trees during

the same period. Although previous studies identified the significance of VPD and precipitation anomaly on an annual timescale (Park Williams *et al.*, 2012), our study uniquely investigates the seasonality of hydraulic vulnerability and carbohydrate storage and their effects on growth – a phenomenon with physiologically and ecologically significant implications as climate changes.

## Materials and Methods

### Plant material

We periodically monitored (*c.* every 4–8 wk) 52 trees of three widely distributed conifer species located in three plots of mixed conifer species separated by a distance of *c.* 0.5–2 km at Challenge Experimental Forest, California, USA. We measured relative water content (RWC), soluble carbohydrates (SC) and starch (St) in *Pseudotsuga menziesii* (Mirb.) Franco ( $n=18$ ), *Pinus ponderosa* Douglas ex C. Lawson ( $n=18$ ), and *Pinus lambertiana* Douglas ( $n=16$ ) trees at 4–8-wk intervals for *c.* 18 months. All trees were 25 yr old and planted on a grid at 2.5 m spacing to minimize the effects of age and stand density. Tree stem diameters, measured at 1.3 m above ground, ranged from 12 to 28 cm, and tree heights were between 13 and 20 m.

### Relative water content

During each visit, we extracted *c.* 25-mm long and 4-mm diameter tissue samples using a tree borer. Cores were extracted from within a 1 m span running lengthwise along the stem, from 0.5 to 1.5 m in height, always facing the same aspect, and avoiding compression and tension wood. Once extracted, tissue samples were immediately placed into a sealed 2-ml centrifuge tube, put in a cooler, returned to the lab, refrigerated at 4°C, and processed within 2 d. We excised and discarded the bark from each tissue sample. Xylem volume was determined from mass displacement of the specimen in a beaker of water on a balance (Borghetti & Edwards, 1991). We then dried the samples at 75°C and reweighed them. Stem RWC was calculated as: 
$$RWC = \frac{M_f - M_d}{(V_f - V_{cw})\rho_{H_2O}} (\rho_{H_2O}, \text{ density of water (g cm}^{-3}\text{)}; M_f \text{ and } M_d, \text{ fresh and dry mass of xylem tissue, respectively (g)}; V_f, \text{ volumetric FW of xylem tissue (g)}; V_{cw}, \text{ volume of cell wall material (m}^3\text{), calculated as } \frac{M_d}{\rho_{cw}} \text{ where } \rho_{cw} \text{ is density of cell wall material, assumed to be } 1.53 \text{ g cm}^{-3} \text{ (Domec \& Gartner, 2001))}.$$

### Nonstructural carbohydrates

With the same trees cores used to measure RWC, we measured soluble carbohydrates in the wood parenchyma cells (i.e. excluding bark and phloem) based on the methods of Leyva *et al.* (2008). In short, 1 ml of deionized water was added to 50 mg of homogenized dried tissue, vortexed, heated to 72°C for 15 min, and spun at 21 000 *g* for 10 min. A 50- $\mu$ l aliquot of the supernatant was diluted ( $\times 25$ ) and mixed with 150  $\mu$ l of sulfuric acid (98%) and anthrone (0.1%, w/v) solution in a 96-well microplate. The precipitated pellet was reserved for later starch

analysis. The plate was cooled on ice ( $<4^{\circ}\text{C}$ ) for 10 min, then heated to  $100^{\circ}\text{C}$  for 20 min, and finally left to adjust to room temperature for 20 min ( $22^{\circ}\text{C}$ ). We determined the sugar concentrations as glucose equivalents from the colorimetric reading (Thermo Fisher Scientific, Waltham, MA, USA) of absorbance at 620 nm (A620) using a predetermined standard curve (0, 0.01, 0.03, 0.1 and  $0.3\text{ mg l}^{-1}$  glucose), and multiplied the outcome by a measured average wood density of  $0.63\text{ g cm}^{-3}$ .

We quantified starch in the remaining pellet using a starch assay kit (STA-20, Sigma-Aldrich) according to a protocol that we modified (JME, FS and OS). First, we washed the pellet twice in 80% (v/v) ethanol, spun it at 21 000 rcf for 10 min, and then disposed of the supernatant. The pellet was digested with  $\alpha$ -amylase and  $\alpha$ -amylglucosidase at  $100^{\circ}\text{C}$  and  $60^{\circ}\text{C}$  incubations for 5 and 15 min, respectively. Finally, we determined the starch concentration by measuring the amount of glucose released by the glucose oxidase-mediated assay (STA-20, Sigma-Aldrich) according to a colorimetric reading at 540 nm (A540) and multiplied the result by wood density resulting in units of  $\text{mg cm}^{-3}$ .

### Branch hydraulic conductivity

For each species, we collected two branches from three different trees at the study site, one from each plot, a total of 18 branches. Branches with needles that appeared healthy were taken from approximately 5 m in height on the south side of each tree. Each branch was measured for relative water content and hydraulic conductivity at three different points in time during bench-top dehydration. To measure hydraulic conductivity we cut a segment from the branch and then recut it under water to *c.* 25 mm length and allowed several minutes for tension relaxation (Wheeler *et al.*, 2013). Driven by a pressure head of 1.96 kPa, we then allowed filtered and degassed water through the branch segment from a mass balance to a water bath. We measured the change in mass over time of the water as it left the mass balance. We calculated sapwood specific hydraulic conductivity ( $K_h$ ) using the length and diameter of the branch segment, the pressure head, and the mass flow of water. Adjacent stem segments were used for calculating RWC as described above. For each species, we then fit a two parameter (i.e.  $\alpha$  and  $\beta$ ) nonlinear equation to relate RWC and  $K_h$ :  $K_h = \alpha \times \text{RWC}^{\beta}$ .

### Tree ring increment

In May, 2016, we took full cores at breast height (1.4 m) for each of the 52 trees examined. We sanded the cores with sandpaper, mounted them on wood plates, scanned them using a flatbed scanner, and used the software package CDENDRO (Larsson, 2003) to semi-automatically calculate ring widths for each core dating from 2015 back to the pith or estimate of pith. Cores were crossdated to account for missing rings. We detrended the ring width series using a standard negative exponential curve in the R library 'DPLR' (Bunn, 2010) to account for expected differences in growth increment due strictly to tree size (Speer, 2010), thereby calculating a ring-width index for each year of each core,

with more positive values associated with higher relative growth rates accounting for tree size. We modeled variation in ring width index as a function of seasonal VPD anomaly and recent precipitation in both summer and winter (see *Statistical model* section below).

### Climatic data

We obtained daily temperature, precipitation and relative humidity data from a Remote Automated Weather Station (RAWS station, Pike County Lookout) located approximately 0.5 to 1.5 km away from the plots. We calculated vapor pressure deficit (VPD) as the difference between saturation vapor pressure (SVP) and actual vapor pressure (AVP), or  $\text{VPD} = \text{SVP} - \text{AVP}$ . SVP is calculated as:  $\text{SVP} = 0.61 \times e^{\frac{17.27 \times T}{T + 237.3}}$ , where  $T$  is temperature ( $^{\circ}\text{C}$ ) (Tetens, 1930). AVP is calculated as:  $\text{AVP} = \text{SVP} \times \frac{\text{RH}}{100}$ , where RH is relative humidity (%).

### Statistical models

Based on the climatic variables above, we tested numerous statistical models to predict RWC. We included random effects for species, plot and tree ID to permit unique responses to VPD and precipitation at each of these levels (see Supporting Information Notes S1 and Methods S1). Ultimately, we selected seasonal VPD anomaly and recent precipitation based on Akaike Information Criteria (AIC) evaluation (see model description above and Methods S1). The significance of fixed effects was assessed using a  $t$ -distribution and estimating the degrees of freedom from the mixed-effects model using the Kenward–Roger approximation in the R package 'PBKRTEST' (Halekoh & Højsgaard, 2014). Linear models relating ring-width index and  $\text{VPD}_{5\text{d,winter}}$ ,  $\text{VPD}_{5\text{d,summer}}$ ,  $\text{P}_{60\text{d,winter}}$  and  $\text{P}_{60\text{d,summer}}$  were run in R using the 'LM' function. All statistical analyses and data used in this manuscript are available as a downloadable folder in Notes S1.

## Results

### California experienced an extreme mid-winter drought in 2015

In early 2015, nearby weather station data (RAWS station, Pike County Lookout) indicated anomalously high mid-winter daily VPD (Fig. 1). January, February and March 2015 had among the highest monthly VPDs on record for those months from 1992 to 2015, at 0.75, 0.65 and 0.83 kPa, respectively – values that approached the mean 1992 to 2014 May VPD of 0.89 kPa (Fig. 1). Additionally, almost no rain occurred in January and March, and February precipitation was slightly below the 1992–2014 median (Fig. 1). This simultaneous occurrence of seasonally high VPD and low precipitation characterized California's 2015 mid-winter drought as highly anomalous. Despite such seasonally unusual conditions, absolute winter VPD values were still more than 50% below even the lowest July and August values (i.e. *c.* 1.9 kPa)—summer months that rarely receive any precipitation (Fig. 1).

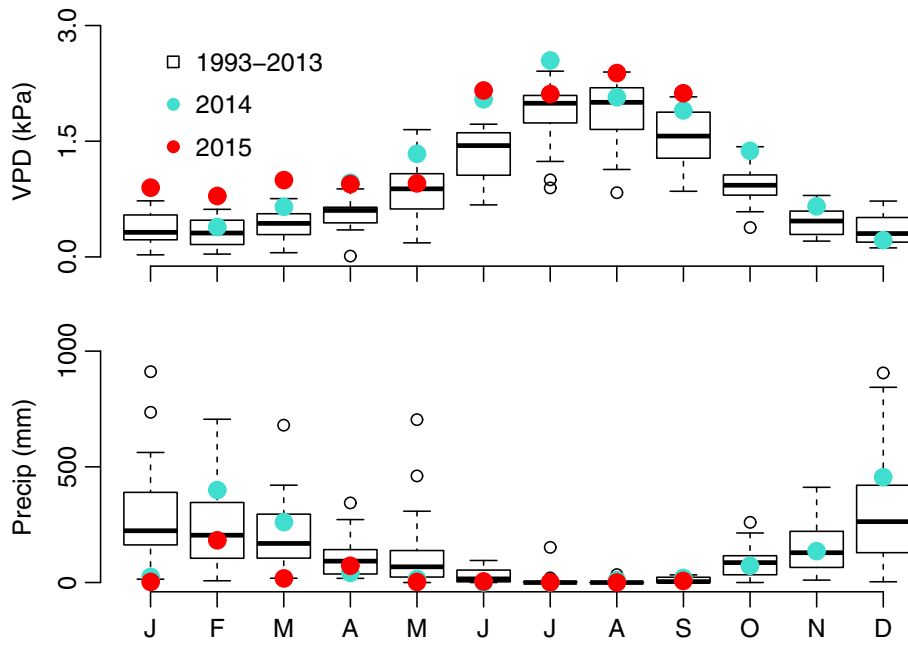


**Fig. 1** Seasonal changes in vapor pressure deficit (VPD, in kPa) and precipitation (precip, in mm). Letters on the x-axis represent each month of the year (January–December). White boxplots represent the median, first and third quartiles. Blue and red points are monthly averages for 2014 and 2015, respectively. Error bars represent the range of observed values excluding outliers (white open circles).

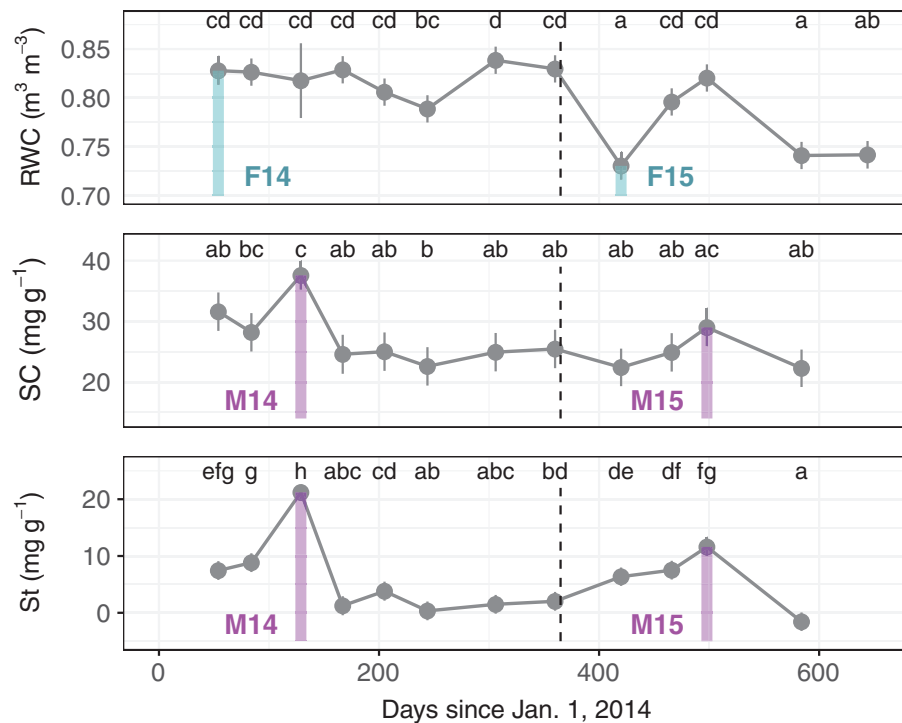


**Fig. 2** Stand-level average values for stem relative water content (RWC), soluble carbohydrates (SC), and starch (St) for *Pseudotsuga menziesii*, *Pinus ponderosa* and *Pinus lambertiana* at various points in time after 1 January 2014 ( $n = 52$ ). Blue bars, RWC during February 2014 (F14) and 2015 (F15), highlighting the significant drop in RWC during February 2015 that corresponded anomalously high VPD and low precipitation. Purple bars, SC and St concentrations in May 2014 (M14) and 2015 (M15), when substantial bud growth and stem lengthening occur. Following the large drop in RWC during February 2015, May 2015 starch concentrations were significantly lower than May 2014. The same characteristic drops in RWC and St were also significant at the species-level (Supporting Information Figs S1–S3). Overlapping letters indicate nonsignificant differences at  $P < 0.05$  based on a Tukey's honest significant difference multiple comparisons test. The black dotted line indicates 31 December 2014.

### Mid-winter drought abruptly reduced stem water content and dampened spring starch accumulation

All three species (*P. menziesii*, *P. ponderosa* and *P. lambertiana*) exhibited seasonal changes in stem relative water content (RWC) during 2014 and 2015 (Fig. 2). Across species, stem RWCs rose by  $0.05 \text{ m}^3 \text{ m}^{-3}$  on average as the characteristic summer drought ended with rainfall beginning October 2014 (Figs 2, S1–S3; Tukey's honest significant difference (HSD),  $P < 0.01$ ). Coincident to the onset of California's anomalous

2015 mid-winter drought, average stem RWC abruptly declined from  $0.84 \text{ m}^3 \text{ m}^{-3}$  in early November 2014 to  $0.73 \text{ m}^3 \text{ m}^{-3}$  in late February 2015 (Fig. 2; Tukey HSD,  $P < 0.01$ ). This pattern of sudden loss in stem RWC was strikingly apparent across all three species. For comparison, individual trees varied substantially in their temporal patterns of RWC during the entire study period, with minimum and maximum values  $0.30$ – $0.99 \text{ m}^3 \text{ m}^{-3}$ . Moreover, certain individuals of each species consistently responded more and less strongly throughout the study period.

Seasonal patterns that were consistent across all three species also were observed for soluble sugar and starch. Soluble sugar concentrations in the stem peaked in May 2014 and again in 2015 (Figs 2, S1–S3), which corresponded with regular stem/branch lengthening and needle expansion. These peaks in May were followed by a sudden drop in soluble sugar into mid-June as the trees entered into seasonal summer drought. Beyond this, soluble sugar concentrations were quite variable from tree to tree and no significant correlation was observed with the mid-winter drought (Fig. 2). Starch concentration peaked in a similar way during May of both years (Figs 2, S1–S3). Across all species, the May peak in both starch (Fig. 2) concentrations was 50% lower in 2015 following the anomalous mid-winter drought compared with 2014 (HSD,  $P < 0.01$ ). This reduced NSC concentration in May 2015 occurred despite VPD being lower than in May 2014, suggesting that VPD limitation of photosynthesis during May 2015 should have been reduced.

### Seasonal, not absolute, VPD anomaly and precipitation corresponded with stem water loss

Recent cumulative precipitation and seasonal VPD anomaly, not the absolute value of VPD, was found to best predict the hydraulic patterns observed (Fig. 3). We tested numerous statistical models using variables derived from recent VPD and precipitation (see Supporting Information Methods S1), as they strongly predict drought-related stress and mortality (Park Williams *et al.*, 2012). Based on AIC, the following model best predicted stem RWC at the stand-level ( $P < 0.05$ ;  $R^2 = 0.72$ ):

$$\text{RWC}_{\text{stem}} = 0.82 + 0.011(P_{60d}) - 0.031(\text{VPD}_{5d}) \quad \text{Eqn 1}$$

( $P_{60}$ , cumulative precipitation in the past 60 d (mm);  $\text{VPD}_{5d}$ , time-series standardization of average VPD during the 5 d before measurement so that values during 1992–2014 have a mean of zero and a standard deviation of one (i.e.  $z$ -score)). Fixed effects in model Eqn 1,  $P_{60}$  and  $\text{VPD}_{5d}$  were significant at  $P < 0.05$  (Fig. S4). Mixed-effect model-explained variance (Xu, 2003), or  $R^2$ , was 0.72. Thus, using only 5-d VPD  $z$ -score anomaly and cumulative precipitation in the previous 60 d, our model explains much of the species- and individual-level responses in RWC – including hydraulic recovery from summer drought into fall and the large loss in stem water content accompanying California’s 2015 mid-winter drought (Fig. 3).

We found a significant nonlinear relationship between branch RWC and  $K_h$  across all three species (Fig. 4;  $K_h = \alpha \times \text{RWC}^\beta$ ;  $P < 0.05$  for parameters  $\alpha$  and  $\beta$ ), defined by the following equations:

$$K_{h,PM} = 1.71 \times \text{RWC}^{3.39} \quad \text{Eqn 2}$$

$$K_{h,PP} = 2.82 \times \text{RWC}^{6.71} \quad \text{Eqn 3}$$

$$K_{h,PL} = 2.42 \times \text{RWC}^{4.23} \quad \text{Eqn 4}$$

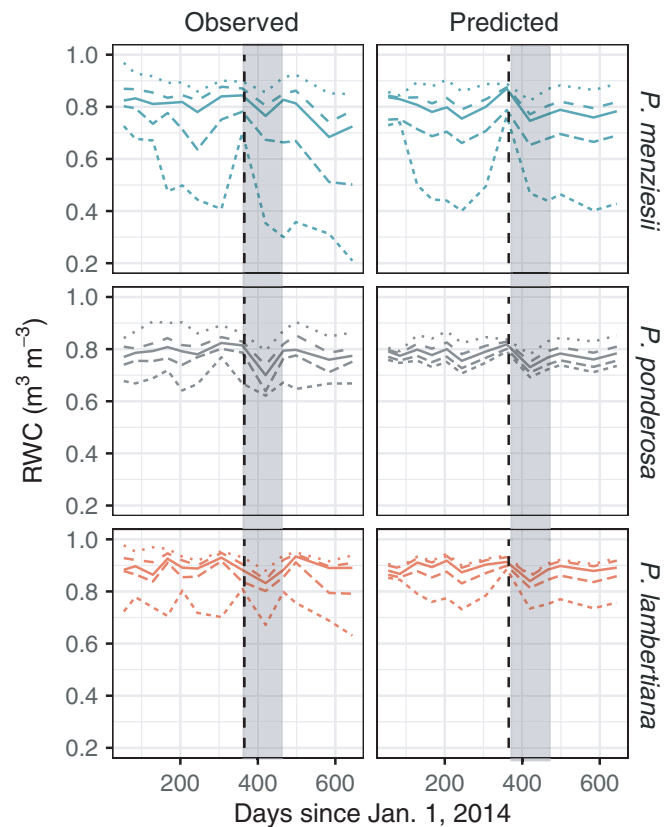


**Fig. 3** Observed and predicted relative water content (RWC) over time for *Pseudotsuga menziesii*, *Pinus ponderosa* and *Pinus lambertiana* ( $n = 18$ ,  $n = 18$ , and  $n = 16$  for each species respectively). The gray bands highlight the mid-winter drought period. Median observed and predicted values are shown with the solid line and surrounded by lines indicating 5<sup>th</sup>, 25<sup>th</sup>, 75<sup>th</sup> and 95<sup>th</sup> observation/prediction intervals in dashed/dotted lines. Predictions were made using the model defined in Eqn 1.

(subscripts PM, PP and PL stand for *P. menziesii*, *P. ponderosa* and *P. lambertiana*, respectively). By March 2015, the average tree had lost 52% hydraulic conductivity, with individual trees rising well above 75%. Caution should be taken when assuming that the relationship between RWC and  $K_h$  can be directly extrapolated to the stem. However, given the difficulty in measuring stem  $K_h$ , such an assumption can facilitate such a comparison.

Based on these relationships and model (Eqn 1), we estimated  $K_h$  of this forest stand over the past 23 yr using measured RWC values for each tree in response to recent and historic climatic data (Figs 5, 6). It is important to note that this exercise does not account for age-related effects on RWC or hydraulic conductance. In comparison to historic climatic events, January, February and March 2015 had among the highest  $\text{VPD}_{5d}$  values and low precipitation in the previous 23-yr period (Fig. 5a). Consequently, the estimated  $K_h$  for all three species was abnormally low during the 2015 mid-winter drought period compared to winter months from 1992 to 2014, and approached or surpassed the average values predicted for summer months from 1992 to 2014 (Fig. 5b).

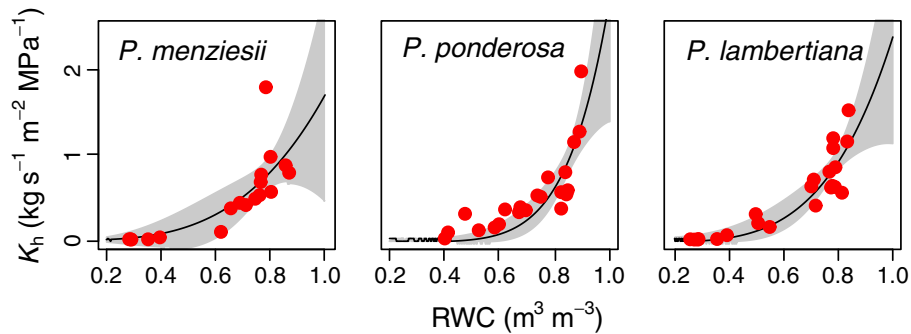


**Fig. 4** Relationship between relative water content (RWC) and hydraulic conductivity ( $K_h$ ) for six branches per species (*Pseudotsuga menziesii*, *Pinus ponderosa* and *Pinus lambertiana*) sampled at multiple time points during bench top dehydration. For each species, we then fit a two parameter (i.e.  $\alpha$  and  $\beta$ ) nonlinear equation to relate RWC and  $K_h$ :  $K_h = \alpha \times \text{RWC}^\beta$ . Parameters for all three species had  $P < 0.05$  ( $n = 18$ ). Confidence intervals are shown in gray bands surrounding the mean estimates (black lines).

### Seasonal, not absolute, VPD anomaly and precipitation corresponded with growth decline

We detected a substantial growth decline based on ring-width index from 2013 through 2015 (Fig. 6c). This growth decline was predicted reasonably well in a multivariate linear model that interacted winter VPD anomaly and winter precipitation ( $R^2 = 0.60$ ; Table S1; see Fig. 7 for individual correlations). However, this growth decline was not predicted well in models based on summer or year-round VPD anomaly or summer or year-round precipitation (Table S1; Fig. 7). Overall, winter VPD anomaly was the strongest individual predictor of growth declines among all variables examined (Fig. 7;  $R^2 = 0.45$ ,  $P \ll 0.01$ ; see Table S1), with 2014 and 2015 having by far the highest winter VPD anomalies and lowest ring-width indices of the 23-yr period, but winter precipitation anomalies that were comparable to six other years in the 23-yr period (2001, 2007–2009 and 2012–2013; Fig. 6).

### Discussion

Ecological drought is defined as moisture limitation in plants resulting from below-average precipitation, above-average

temperature, or especially both (Clark *et al.*, 2016). Implicit in this definition is the critical importance of seasonality in defining temperature and precipitation anomalies, particularly in such climates as Mediterranean and monsoonal regions where there are distinct and predictable seasonal cycles in climate. If above average temperatures and below average precipitation occur at different times of year, or at times where plants are dormant, then simple annual climatic averages may fail to capture meaningful ecological drought. Here we document a strong seasonal signal in how plant physiology responds to drought, with implications for tree vitality. By parameterizing species-specific relationships between recent climate and stem relative water content (RWC), and between RWC and hydraulic conductivity ( $K_h$ ), we demonstrate that the risk of hydraulic loss and starch accumulation in conifer trees during periods of low precipitation is dependent on the seasonal anomaly in vapor pressure deficit (VPD) rather than the absolute VPD. In the montane Mediterranean climate of California where conifer photosynthesis can occur year round, winter VPDs that are higher than average but still lower than summer VPDs appear to be an important causal factor inducing tree water stress.

A tree's vitality and photosynthetic capacity are tightly linked to its vascular system's ability to transport water: its hydraulic conductivity. A tree with high conductivity would permit greater

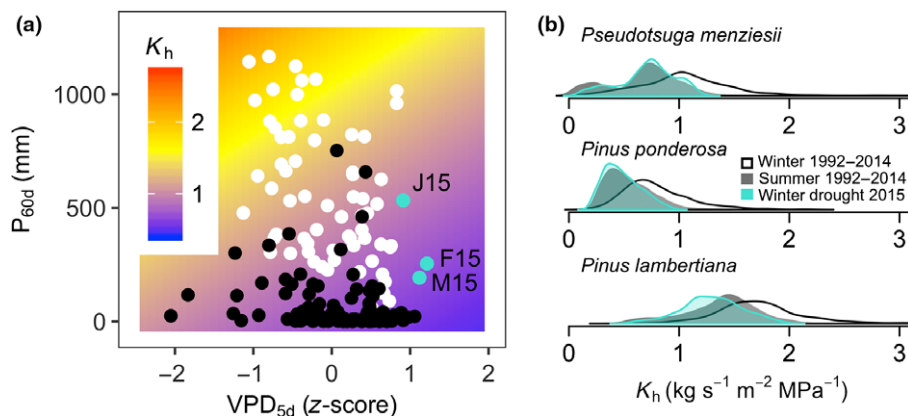


**Fig. 5** (a) Predicted stand-level hydraulic conductivity ( $K_h$ ) in response to seasonal vapor pressure deficit (VPD) anomaly, inter-annual VPD anomaly ( $\text{VPD}_{5d}$ ), and cumulative 60-d precipitation ( $P_{60d}$ ). Median monthly  $\text{VPD}_{5d}$  and  $P_{60d}$  values from 1992 to 2014 are plotted for summer (black dots) and winter (white dots). Values for winter drought 2015, January (J15), February (F15) and March (M15) are shown using turquoise dots. (b) Probability density curves for tree-level daily estimated  $K_h$  from 1992 to 2015 for summer (gray shaded area), winter (white shaded area), and 2015 winter drought months (turquoise shaded area, January, February and March).

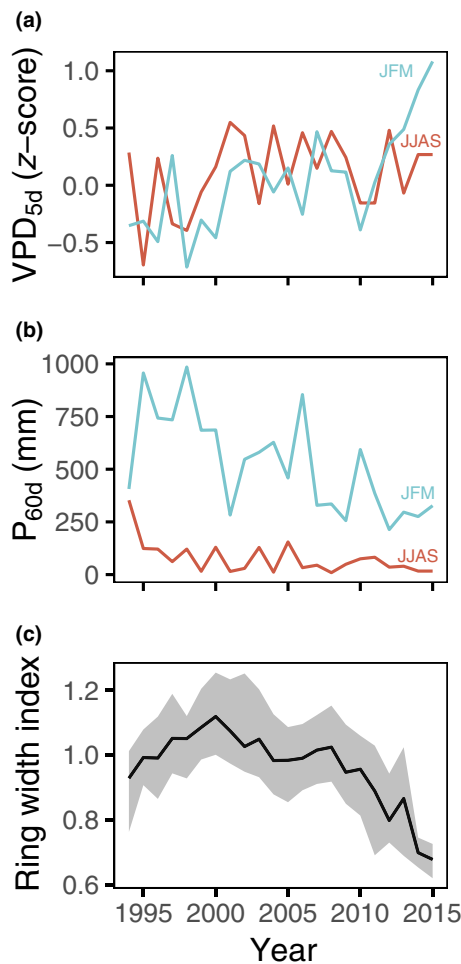


**Fig. 6** (a) Temporal trends in inter-annual vapor pressure deficit (VPD) anomaly for January, February and March ( $VPD_{5d,winter}$ ; solid blue line) and June, July, August and September ( $VPD_{5d,summer}$ ; solid red line) from 1993 to 2015. (b) Temporal trends in cumulative 60-d precipitation for January, February and March ( $P_{60d,winter}$ ; solid blue line) and June, July, August and September ( $P_{60d,summer}$ ; solid red line) from 1993 to 2015. (c) Temporal trends in stand-level average annual ring-width index from 1993 to 2015. Confidence intervals are shown in gray bands surrounding the mean estimates (black solid line).

water flow for a given pressure gradient. Percentage loss of hydraulic conductivity (PLC), relative to the maximum, is commonly used to describe plant hydraulic status, where the likelihood of mortality due to drought increases with PLC (Anderegg

*et al.*, 2013; Adams *et al.*, 2017). Though often overlooked, conifers show a strong relationship between hydraulic conductivity and RWC (Domec & Gartner, 2001, 2002, 2003). In this study, we likewise find support for this relationship in three widely distributed conifer species. Thus, by estimating  $K_h$  from RWC values (which are more easily measurable in the field), we are able to meaningfully assess tree hydraulic status. Based on our model, we estimate that the 2015 mid-winter drought resulted in among the largest stand-level losses in hydraulic conductivity since at least 1992 (Fig. 4), on the order of 50%. In comparison to historic summer and winter ranges, we estimate that January to March 2015 induced extreme levels of hydraulic loss, which may border along critical thresholds of hydraulic conductivity loss associated with tree mortality (Adams *et al.*, 2017).

The large drop in  $K_h$  (*c.* 50%) during severe mid-winter drought was followed by reduced concentrations of starch the following spring (also *c.* 50%) relative to the previous year (Fig. 2). This reduced accumulation of starch does not appear to be associated with springtime drought stress, as the VPD anomaly and precipitation in the previous 60 d before the May 2015 measurement was about average (Fig. 1), and stem RWC returned to pre-drought levels (Fig. 2). We suggest instead that the reduction in spring starch concentration may be the result of either (1) consumption of starch reserves during the mid-winter drought to maintain basic metabolic function during a period of stomatal closure, and/or (2) a legacy of impaired hydraulic conductivity during the mid-winter drought, where the tree must ‘catch up’ on growth and structural carbohydrate allocation during the spring and has less reserve energy to devote to starch production. Whatever the case, the decrease in spring starch concentrations and the subsequent complete depletion of starch in summer 2015 (Fig. 2) suggest that that mid-winter drought may also compromise NSCs and potentially contribute to reduced vitality/productivity in the following summer or increased tree morbidity via carbon starvation in addition to hydraulic failure (McDowell *et al.*, 2008). It is important, however, that future studies investigate a longer time series of physiological data and in more controlled experimental conditions.

It is likely that the unprecedentedly high VPD in winter 2014 and 2015, coinciding with anomalously low winter precipitation, led to a period of stomatal closure that reduced hydraulic conductivity, depleted carbohydrate stores for metabolism, and caused the signal of reduced secondary growth that we observed

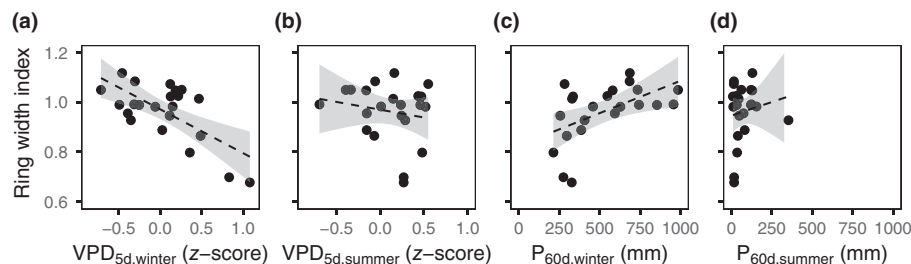


**Fig. 7** Linear relationships of ring-width index with (a) vapor pressure deficit (VPD) anomaly for January, February and March ( $VPD_{5d,winter}$ ), (b) VPD anomaly for June, July, August and September ( $VPD_{5d,summer}$ ), (c) cumulative 60-d precipitation for January, February and March ( $P_{60d,winter}$ ), and (d) cumulative 60-d precipitation for June, July, August and September ( $P_{60d,summer}$ ). Confidence intervals are shown in grey bands surrounding the mean estimates (black dotted lines). Statistical parameters for the linear models are provided in Supporting Information Table S1.

in the ring-width data (Fig. 6). At these lower elevations, conifers may be photosynthesizing year-round (Kelly & Goulden, 2016), and thus may be acclimatized to ample precipitation and mild VPD to support that growth. We appear to have observed an interruption in that growth that is directly associated with both decreased hydraulic conductivity and decreased carbohydrate accumulation during winter photosynthesis (Fig. 2). This decreased growth, while not directly associated with mortality in our study, could partially explain decreases in forest productivity under hotter drought (Zhao & Running, 2010), and may explain the physiological mechanisms underlying mortality patterns in regions where average climate is hotter and drier than at our study site and trees may be closer to their physiological limits (Young *et al.*, 2017).

Given anticipated changes in climate this century, more intense winter drought could amplify hydraulic loss in forests. Global temperatures are rising in association with increased concentrations of atmospheric CO<sub>2</sub>. California experienced a 1.0°C increase in average temperature from 1970 to 2006 (Cordero *et al.*, 2011), which is predicted to rise 1.5–4.5°C by the end of the 21<sup>st</sup> Century (Cayan *et al.*, 2008). For a given relative humidity, greater temperature increases transpirational demand and ultimately embolism formation by increasing VPD. Thus, in upcoming decades the co-occurrence of a dry winter with warmer days would result in higher VPD. Our findings suggest that if climate change elevates winter VPD, conifers may be increasingly vulnerable to winter stem hydraulic loss. Much uncertainty exists about future precipitation patterns in California (Cayan *et al.*, 2008), which limits our ability to predict winter drought frequency and severity. Increased future precipitation could buffer winter hydraulic loss due to anomalously high VPD, or decreased future precipitation could exacerbate hydraulic loss. Although our dataset is limited in temporal coverage, historic weather patterns at our field site from 1992 to 2015 align with the trend of increasing winter VPD and decreasing winter precipitation (Fig. 5).

Loss in hydraulic conductivity due to xylem embolism formation is driven by the water potential to which a plant is exposed – high atmospheric VPD and low soil water potential induces embolism formation and decreases hydraulic conductivity (Tyree & Sperry, 1989). As a result, summer drought has been the focus of past studies on hydraulic failure. Winter is notable for embolism formation due to freezing (Sperry & Sullivan, 1992), but has not been previously considered as a source of drought-related embolism formation. Here, we show that a substantial loss of hydraulic conductivity can occur even during winter months, in the absence of freezing temperatures (Fig. S5) and despite relatively low VPD in comparison to summer values (Fig. 1). This seasonal hydraulic vulnerability links to seasonal phenology and should be taken into account in investigations of plant physiology. Differences in hydraulic properties between earlywood and latewood offer one possible explanation for such a phenomenon. Earlywood embolizes at lower tension than latewood (Domec & Gartner, 2002) and, thus, the timing of earlywood and latewood growth could lead to greater winter vulnerability. Alternatively, seasonal changes in stomatal sensitivity of evergreen species could affect the rate of stem water loss.

Such a phenomenon would require that stomata are less sensitive to water potential during winter, which would align with observations that conifer stomata are more responsive to VPD (or local epidermal water potential) than to xylem water potential (Zwieniecki *et al.*, 2007). Other explanations such as less suberized roots or less cutinized leaves (i.e. higher epidermal conductance) due to winter or spring growth could also explain increased winter susceptibility to loss in conductivity. At this point, however, these explanations are speculative. Manipulative studies will be required to determine the physiology underlying winter drought-induced loss in hydraulic conductivity and to determine its ecological impact on forest vitality as climate changes.

## Acknowledgements

During the period of this research J.M.E. received funding through the US Environmental Protection Agency STAR fellowship program as a doctoral student at University of California Davis. Amanda Soares de Soza provided invaluable assistance in processing samples and discussing results.

## Author contributions

J.M.E. collected and analyzed samples, built the statistical models, and wrote the manuscript; J.T.S., M.P.N. and M.A.Z. assisted with writing the manuscript; O.S. assisted with analyzing samples and writing the manuscript; and J.O. assisted with analyzing samples.

## ORCID

J. Mason Earles  <http://orcid.org/0000-0002-8345-9671>  
Jens T. Stevens  <http://orcid.org/0000-0002-2234-1960>

## References

- Adams HD, Zeppel MJB, Anderegg WRL, Hartmann H, Landhäusser SM, Tissue DT, Huxman TE, Hudson PJ, Franz TE, Allen CD *et al.* 2017. A multi-species synthesis of physiological mechanisms in drought-induced tree mortality. *Nature Ecology & Evolution* 1: 1285–1291.
- Allen CD, Breshears DD. 1998. Drought-induced shift of a forest–woodland ecotone: rapid landscape response to climate variation. *Proceedings of the National Academy of Sciences, USA* 95: 14839–14842.
- Allen CD, Breshears DD, McDowell NG. 2015. On underestimation of global vulnerability to tree mortality and forest die-off from hotter drought in the Anthropocene. *Ecosphere* 6: 1–55.
- Allen CD, Macalady AK, Chenchouni H, Bachelet D, McDowell N, Venetier M, Kitzberger T, Rigling A, Breshears DD, Hogg EH *et al.* 2010. A global overview of drought and heat-induced tree mortality reveals emerging climate change risks for forests. *Forest Ecology and Management* 259: 660–684.
- Anderegg WRL, Berry JA, Smith DD, Sperry JS, Anderegg LDL, Field CB. 2012. The roles of hydraulic and carbon stress in a widespread climate-induced forest die-off. *Proceedings of the National Academy of Sciences, USA* 109: 233–237.
- Anderegg WRL, Plavcová L, Anderegg LDL, Hacke UG, Berry JA, Field CB. 2013. Drought's legacy: multiyear hydraulic deterioration underlies widespread aspen forest die-off and portends increased future risk. *Global Change Biology* 19: 1188–1196.



- Borghetti M, Edwards W. 1991. The refilling of embolized xylem in *Pinus sylvestris* L. *Plant, Cell & Environment* 14: 357–369.
- Breshears DD, Myers OB, Meyer CW, Barnes FJ, Zou CB, Allen CD, McDowell NG, Pockman WT. 2009. Tree die-off in response to global change-type drought: mortality insights from a decade of plant water potential measurements. *Frontiers in Ecology and the Environment* 7: 185–189.
- Bunn AG. 2010. Statistical and visual crossdating in R using the dplR library. *Dendrochronologia* 28: 251–258.
- Cayan DR, Maurer EP, Dettinger MD, Tyree M, Hayhoe K. 2008. Climate change scenarios for the California region. *Climatic Change* 87: 21–42.
- Clark JS, Iverson L, Woodall CW, Allen CD, Bell DM, Bragg DC, D'Amato AW, Davis FW, Hersh MH, Ibanez I *et al.* 2016. The impacts of increasing drought on forest dynamics, structure, and biodiversity in the United States. *Global Change Biology* 22: 2329–2352.
- Cordero EC, Kessomkiat W, Abatzoglou J, Mauget SA. 2011. The identification of distinct patterns in California temperature trends. *Climatic Change* 108: 357–382.
- Domec J-C, Gartner BL. 2001. Cavitation and water storage capacity in bole xylem segments of mature and young Douglas-fir trees. *Trees* 15: 204–214.
- Domec J-C, Gartner BL. 2002. How do water transport and water storage differ in coniferous earlywood and latewood? *Journal of Experimental Botany* 53: 2369–2379.
- Domec J-C, Gartner BL. 2003. Relationship between growth rates and xylem hydraulic characteristics in young, mature and old-growth ponderosa pine trees. *Plant, Cell & Environment* 26: 471–483.
- Fellows AW, Goulden ML. 2012. Rapid vegetation redistribution in Southern California during the early 2000s drought. *Journal of Geophysical Research* 117: G03025.
- Halekoh U, Højsgaard S. 2014. A Kenward-Roger approximation and parametric bootstrap methods for tests in linear mixed models – the R package pbkrtest. *Journal of Statistical Software* 59: 1–32.
- Jensen KH, Berg-Sørensen K, Bruus H, Holbrook NM, Liesche J, Schulz A, Zwieniecki MA, Bohr T. 2016. Sap flow and sugar transport in plants. *Review of Modern Physics* 88: 35007.
- Keeley J, Sypard A. 2016. Climate change and future fire regimes: examples from California. *Geosciences* 6: 37.
- Kelly AE, Goulden ML. 2016. A montane Mediterranean climate supports year-round photosynthesis and high forest biomass. *Tree Physiology* 36: 459–468.
- Larsson L-A. 2003. *CDendro (version 8.0)*. [WWW document] URL <http://www.cybis.se/forfun/dendro> [accessed 15 January 2017].
- Leyva A, Quintana A, Sánchez M, Rodríguez EN, Cremata J, Sánchez JC. 2008. Rapid and sensitive anthrone-sulfuric acid assay in microplate format to quantify carbohydrate in biopharmaceutical products: method development and validation. *Biologicals: Journal of the International Association of Biological Standardization* 36: 134–141.
- McDowell N, Pockman WT, Allen CD, Breshears DD, Cobb N, Kolb T, Plaut J, Sperry J, West A, Williams DG *et al.* 2008. Mechanisms of plant survival and mortality during drought: why do some plants survive while others succumb to drought? *New Phytologist* 178: 719–739.
- Menne M, Durre I, Korzeniewski B, McNeal S, Thomas K, Yin X, Anthony S, Ray R, Vose R, Gleason B *et al.* 2015. *Global historical climatology network - daily (GHCN-daily), version 3.15*. NOAA National Climatic Data Center. [WWW document] URL <http://doi.org/10.7289/V5D21VHZ> [accessed December 2015].
- Millar CI, Stephenson NL. 2015. Temperate forest health in an era of emerging megadisturbance. *Science* 349: 823–826.
- van der Molen MK, Dolman AJ, Ciais P, Eglin T, Gobron N, Law BE, Meir P, Peters W, Phillips OL, Reichstein M *et al.* 2011. Drought and ecosystem carbon cycling. *Agricultural and Forest Meteorology* 151: 765–773.
- Nardini A, Battistuzzo M, Savi T. 2013. Shoot desiccation and hydraulic failure in temperate woody angiosperms during an extreme summer drought. *New Phytologist* 200: 322–329.
- Park Williams A, Allen CD, Macalady AK, Griffin D, Woodhouse CA, Meko DM, Swetnam TW, Rauscher SA, Seager R, Grissino-Mayer HD *et al.* 2012. Temperature as a potent driver of regional forest drought stress and tree mortality. *Nature Climate Change* 3: 292–297.
- Robeson SM. 2015. Revisiting the recent California drought as an extreme value. *Geophysical Research Letters* 42: 6771–6779.
- Sevanto S, McDowell NG, Dickman LT, Pangle R, Pockman WT. 2014. How do trees die? A test of the hydraulic failure and carbon starvation hypotheses. *Plant, Cell & Environment* 37: 153–161.
- Speer JH. 2010. *Fundamentals of tree ring research*. Tuscon, AZ, USA: University of Arizona Press.
- Sperry JS, Sullivan JE. 1992. Xylem embolism in response to freeze-thaw cycles and water stress in ring-porous, diffuse-porous, and conifer species. *Plant Physiology* 100: 605–613.
- Tetens O. 1930. Über einige meteorologische Begriffe. *Geophys* 6: 297–309.
- Tyree MT, Sperry JS. 1989. Vulnerability of xylem to cavitation and embolism. *Annual Review of Plant Physiology and Plant Molecular Biology* 40: 19–38.
- Wheeler JK, Huggett BA, Tofte AN, Rockwell FE, Holbrook NM. 2013. Cutting xylem under tension or supersaturated with gas can generate PLC and the appearance of rapid recovery from embolism. *Plant, Cell & Environment* 36: 1938–1949.
- Williams AP, Seager R, Abatzoglou J, Cook B, Smerdon J, Cook E. 2015. Contribution of anthropogenic warming to California drought during 2012–2014. *Geophysical Research Letters* 42: 6819–6828.
- Xu R. 2003. Measuring explained variation in linear mixed effects models. *Statistics in Medicine* 22: 3527–3541.
- Young DJN, Stevens JT, Earles JM, Moore J, Ellis A, Jirka AL, Latimer AM. 2017. Long-term climate and competition explain forest mortality patterns under extreme drought. *Ecology Letters* 20: 78–86.
- Zhao M, Running SW. 2010. Drought-induced reduction in global terrestrial net primary production from 2000 through 2009. *Science* 329: 940–943.
- Zwieniecki MA, Brodrick TJ, Holbrook NM. 2007. Hydraulic design of leaves: insights from rehydration kinetics. *Plant, Cell & Environment* 30: 910–921.

## Supporting Information

Additional Supporting Information may be found online in the Supporting Information tab for this article:

**Fig. S1** Time-series of relative water content for stand- and species-level.

**Fig. S2** Time-series of soluble sugar concentration for stand- and species-level.

**Fig. S3** Time-series of starch concentration for stand- and species-level.

**Fig. S4** Median fixed effect and random effect parameter estimates relating climatic variables to relative water content.

**Fig. S5** Histogram showing daily minimum temperature in January, February and March of 2015.

**Table S1** Parameter estimates, standard errors, *P*-values and *R*<sup>2</sup> values for linear models relating ring-width index and select climatic variables

**Methods S1** Supporting methods for manuscript.

**Notes S1** R code and data used for statistical modeling.

Please note: Wiley Blackwell are not responsible for the content or functionality of any Supporting Information supplied by the authors. Any queries (other than missing material) should be directed to the *New Phytologist* Central Office.